

MIT Open Access Articles

Anion Exchange Membranes: Enhancement by Addition of Unfunctionalized Triptycene Poly(Ether Sulfone)s

The MIT Faculty has made this article openly available. **Please share** how this access benefits you. Your story matters.

Citation: Kim, Yoonseob et al. "Anion Exchange Membranes: Enhancement by Addition of Unfunctionalized Triptycene Poly(Ether Sulfone)s." ACS Applied Materials & Interfaces 9, 49 (December 2017): 42409–42414 © 2017 American Chemical Society

As Published: <http://dx.doi.org/10.1021/ACSAMI.7B13058>

Publisher: American Chemical Society (ACS)

Persistent URL: <http://hdl.handle.net/1721.1/119624>

Version: Author's final manuscript: final author's manuscript post peer review, without publisher's formatting or copy editing

Terms of Use: Article is made available in accordance with the publisher's policy and may be subject to US copyright law. Please refer to the publisher's site for terms of use.



1
2
3
4
5
6
7
8
9
10
11
12
13
14
15
16
17
18
19
20
21
22
23
24
25
26
27
28
29
30
31
32
33
34
35
36
37
38
39
40
41
42
43
44
45
46
47
48
49
50
51
52
53
54
55
56
57
58
59
60

Anion Exchange Membranes: Enhancement by Addition of Unfunctionalized Triptycene Poly(Ether Sulfone)s

*Yoonseob Kim[‡], Lionel C.H. Moh[‡] and Timothy M. Swager**

Department of Chemistry, Massachusetts Institute of Technology, Cambridge, MA 02139 USA

KEYWORDS. anion exchange membrane, triptycene copolymer, phase separation, hydroxide conductivity, mechanical property

Abstract

Anion exchange membrane fuel cells are a clean and efficient promising future energy source. However, the development of stable high performance membranes remains a major challenge. Herein we demonstrate that the addition of unfunctionalized triptycene poly (ether sulfones) into 1-methylimidazolium poly (ether sulfone) enhances membrane's conductivity (up to 0.082 S/cm at 80 °C), minimizes dimensional changes over temperatures from 20 °C to 80 °C, and enhances stability with 30% of the initial conductivity maintained after 450 h. These enhancements appear to be the result of nano-phase separation and internal free volume. Small angle X-ray scattering

1
2
3 and transmission electron microscopy reveal that the internal domain size increases (up to 7.44
4 nm) with increasing triptycene fraction.
5
6
7
8
9

10
11
12 The anion exchange membrane fuel cell (AEMFC) is an electrochemical device that can
13 converts the chemical energy of H₂ (or methanol) directly into an electrical current. Interest in
14 anion exchange membrane fuel cells have been driven by the environmentally friendly nature of
15 these systems, the higher oxygen reduction reaction kinetics relative to proton exchange
16 membrane fuel cells, lower methanol permeability through the membranes in alkaline media, and
17 the fact that the earth abundant metals are efficient fuel cell catalysts under basic conditions.¹⁻³
18 However, there are impediments to the adoption of AEMFCs. In particular efficiency and
19 stability of the anion exchange membranes (AEMs) remains a weakness. A typical alkaline
20 AEM is composed of a polymer backbone with tethered cationic ion-exchange groups to
21 facilitate the movement of free OH⁻ ions, while being impermeable to cations. The challenge is
22 to fabricate AEMs with high OH⁻ ion conductivity and mechanical durability without chemical
23 degradation at elevated temperatures and pH.⁴
24
25
26
27
28
29
30
31
32
33
34
35
36
37
38
39

40 Cationic polymers based on poly(arylene ether sulfone), polyphenylenes,
41 polybenzimidazole, poly(epichlorohydrins) and polyethylene have been extensively studied as
42 AEMs.⁵⁻¹⁰ Among them, poly(arylene ether sulfone)s (PES) as base polymers have received the
43 most attention due to their excellent thermal, mechanical and chemical stability. Furthermore, a
44 wide range of functionalization chemistry has been developed for these materials and thus, PES
45 has emerged as a versatile candidate for development of AEM.¹¹ Even though potentially
46 weaker stability is predicted as a result of nucleophilic attack on cation functionalized
47 backbones,¹² numerous efforts on quaternary ammonium with different chemical structures as
48
49
50
51
52
53
54
55
56
57
58
59
60

1
2
3 cation functional groups have been shown to exhibit alkaline stability and high ion
4 conductivity.^{4,13,14} Of these groups, the methyl imidazolium structure is particularly attractive as
5
6 a result of its OH⁻ conductivity and chemical stability resulting from its five-membered aromatic
7
8 ring structure. The electronic delocalization within the rings diffuses charge density of a cation
9
10 and thereby weakens electrostatic interactions with the hydroxide ions to prevent strong pinning
11
12 and facilitate higher conductivity.¹⁵ Furthermore, the absence of a sp³ environment and β-
13
14 hydrogens removes the possibility of elimination reactions.^{3,16} In order to utilize the
15
16 imidazolium functional group to its maximum potential in PES, high degrees of functionalization
17
18 have been pursued. However, at high degrees of functionalization, imidazolium bisphenol A PES
19
20 (Im-BPAPES) was not mechanically stable as a result of swelling and dissolution. Improvement
21
22 strategies to create mechanically stable imidazolium containing membranes include the design of
23
24 comb-shaped polymers,¹⁷ block copolymers,^{18,19} and crosslinking.²⁰ These methods utilize
25
26 nanoscale hydrophobic/hydrophilic phase separations to drive the formation of interconnected
27
28 ion conducting channels while maintaining mechanical stability.^{21,22}

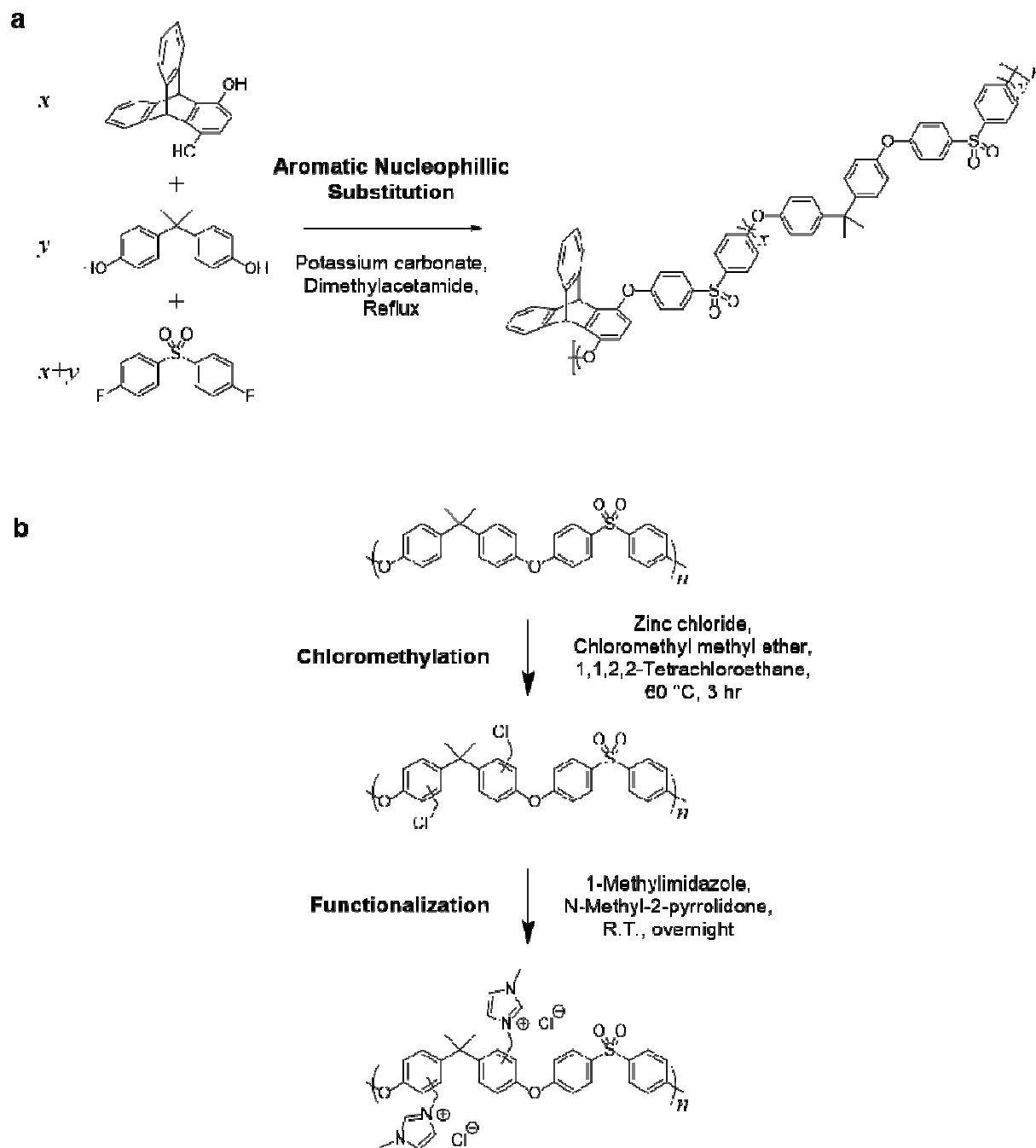
29
30
31
32
33
34
35
36
37 Herein we introduce a new and facile way to enhance ion conductivity, mechanical
38
39 stability and chemical stability simultaneously by using triptycene-containing PES as an additive.
40
41 Triptycene is known to enhance polymer properties by the translation of its unique molecular
42
43 characteristics to bulk systems. Specifically its rigid 3D structure promotes high internal free-
44
45 volume that prevents dense packing of molecular chains and an interlocked structure, creating
46
47 materials with high glass transition temperatures and enhanced mechanical properties.²³
48
49 Examples of the utility of triptycenes in polymers include creating materials with size exclusion
50
51 properties and high fluorescence,²⁴ producing low dielectric constant solids,²⁵ and the
52
53 simultaneous enhancement of ductility and stiffness of films and fibers.²⁶ Our expectation is that
54
55
56
57
58
59
60

1
2
3 some of these attractive attributes can be transferred to AEMs by blending. This is not the first
4 realization that including triptycenes in a polymer's backbone can improve an anion conducting
5 membrane.²⁷ However we are taking a different approach by exploring if the addition of an
6 unfunctionalized triptycene PES will improve AEM properties.
7
8
9
10
11

12 High conductivity of hydroxide ions at working temperatures (60-80 °C) are a
13 requirement for viable high-performance fuel cells. The two major parameters which determine
14 hydroxide conductivity of membrane are the ion exchange capacity (IEC) and the internal
15 domain structure that affects ion mobility. In this study, the IEC is designed to be constant for all
16 samples, allowing for a direct observation of the effect of triptycene additives on the ion mobility
17 through changes in the material's internal domain structure. It is generally accepted that
18 increased ion conductivity at higher temperatures is a result of an expansion of the free volume
19 in the polymer membrane.²⁸ As a result, we rationalized that the addition of free volume
20 promoting triptycene groups in the materials will enhance hydroxide conduction relative to pure
21 Im-BPAPES membranes.
22
23
24
25
26
27
28
29
30
31
32
33
34
35

36 As indicated, BPAPES is an established material from which AEMs were made and
37 hence is well suited to test our hypothesis. Post-polymerization reactions provide randomly-
38 functionalized BPAPES that is expected to have a homogenous solid state structure when made
39 into a film. As a first step, highly chloromethylated BPAPES (Cl-BPAPES) was synthesized
40 (Scheme 1). The degree of chloromethylation was found to be 95% by ¹H NMR spectroscopy
41 (Supporting Information Figure S1). Cl-BPAPES was then reacted with 1-methylimidazole to
42 form 1-methylimidazolium BPAPES (Im-BPAPES). Im-BPAPES was cast into a free-standing
43 membrane and repeatedly soaked in fresh solutions of 1.0 M sodium hydroxide to yield an
44 alkaline AEM with OH⁻ ions and an IEC of 2.40 mmol/g (See SI for details of sample
45
46
47
48
49
50
51
52
53
54
55
56
57
58
59
60

1
2
3 preparation). To study the effect of additives on conductivity and properties of the films,
4 unfunctionalized triptycene containing PES copolymers (TrpPES) as well as unfunctionalized
5 BPAPES were combined with Im-BPAPES in AEMs. By design we have kept the fractional
6 mass of the Im-BPAES constant in all films. In this way, the IEC of the samples are constant,
7 and the effect of additive polymers can be directly observed. To control the free volume
8 introduced by the additives, PESs with five different ratios of bisphenol A and triptycene-1,4,-
9 hydroquinone were used: BPAPES, TrpPES(1,4), TrpPES(1,1), TrpPES(4,1), and TrpPES(1,0)
10 (Scheme 1, Table S1 and Table S2). TrpPES(1,0) contains the most triptycene functional group
11 and it is expected that this material would impart the greatest amount of internal free volume into
12 the membrane. Membranes were formed from solutions containing a fixed mass of Im-BPAPES
13 and the same weight of each additive BPAPES, TrpPES(1,4), TrpPES(1,1), TrpPES(4,1), and
14 TrpPES(1,0). The polymer solutions were then cast to form AEMs with different amounts of
15 triptycene: TRP-0, TRP-20, TRP-50, TRP-80, and TRP-100, respectively (Table S2). Im-
16 BPAPES from a single reaction batch was used to ensure that all five AEMs have the same IECs
17 of 1.83 ± 0.05 mmol/g (See SI for details of sample preparation).
18
19
20
21
22
23
24
25
26
27
28
29
30
31
32
33
34
35
36
37
38
39
40
41
42
43
44
45
46
47
48
49
50
51
52
53
54
55
56
57
58
59
60



Scheme 1. **a.** Synthesis of TrpPES copolymer. Ratios between x and y are represented as (x,y) in TrpPES(x,y) and five different copolymers were synthesized. The ratios of (0,1), (1,4), (1,1), (4,1) and (1,0) gave BPAPES, TrpPES(1,4), TrpPES(1,1), TrpPES(4,1), and TrpPES(1,0), respectively (Table S1 and S2). **b.** Synthesis of Im-BPAPES copolymer from chloromethylation of BPAPES.

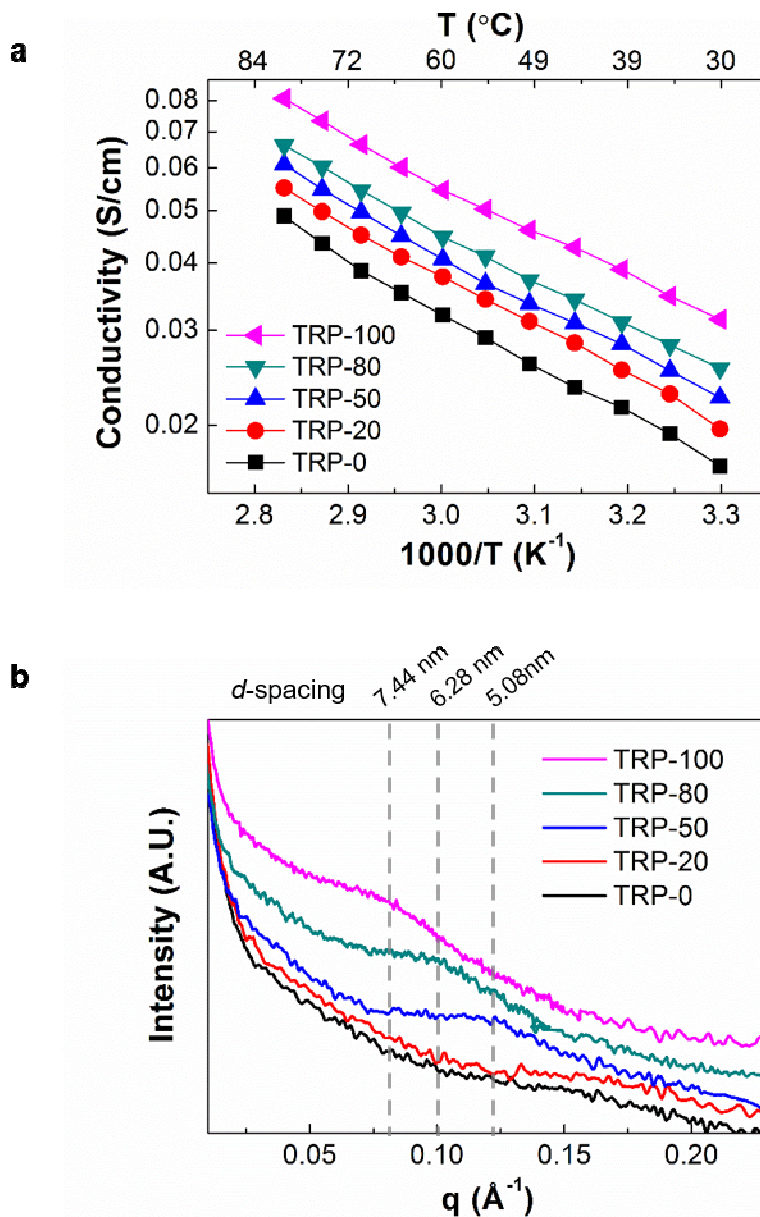


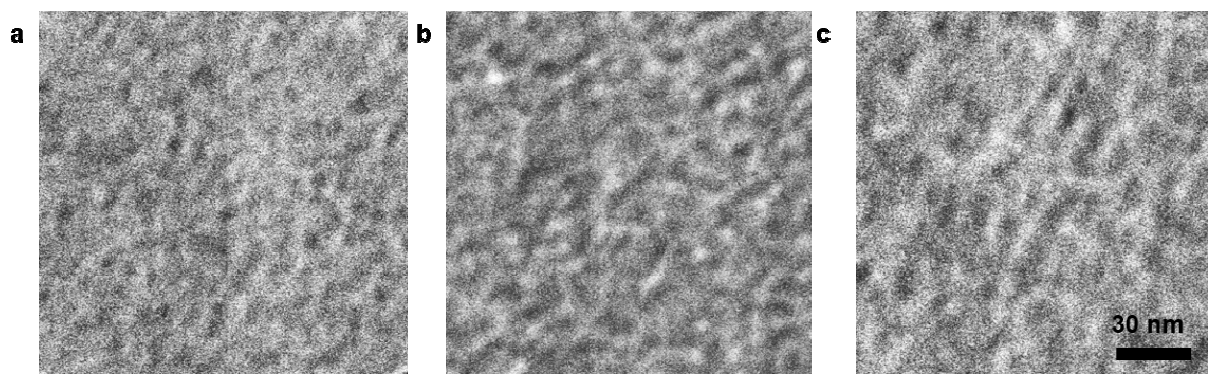
Figure 1. a. Temperature dependent conductivity of samples. All samples had IEC of 1.82 ± 0.05 mmol/g. b. SAXS spectra of the samples. *d*-spacing values for TRP-50, -80 and -100 were calculated to be 5.08, 6.28 and 7.44 nm.

Temperature-dependent hydroxide conductivities were measured for the different compositions (Figure 1a). Without any triptycene groups in the additive polymer, TRP-0 has a conductivity of 0.018 S/cm at 20 °C. On the other hand, using TrpPES(1,0) as an additive, TRP-100 displayed an increased conductivity of 0.030 S/cm at the same temperature. At a higher

1
2
3 temperature of 80 °C, TRP-100's conductivity is 0.082 S/cm, which is 1.7-times higher than
4 conductivity of TRP-0 at the same temperature. Conductivities of the AEMs at working
5 temperatures (60 – 80 °C) surpassed the required conductivity of 0.05 S/cm that is considered
6 necessary for reliable performance, and the fact that membranes of TRP-100 performed close to
7 0.1 S/cm which is often regarded as prerequisite for high performance cell output⁴ is promising.
8 Furthermore, the TRP-100 AEM displays a higher conductivity than previously reported
9 triptycene poly(arylene ether sulfone)s derived materials with 0.072 S/cm at 80 °C and a higher
10 IEC of 2.61 mmol/g.²⁷ Our results suggest that balancing free volume and IEC is more important
11 than simply having a higher IEC. Furthermore TRP-100 displays an record conductivity for an
12 AEMs based on BPAPES.^{16,29,30} The conduction behavior of the samples over the temperature
13 range of 20 – 80 °C obeyed Arrhenius behavior with the R² linear regression values in excess of
14 0.99 for all samples (Figure S3). Activation energies, E_a, which reveal the minimum activation
15 energies for conduction were calculated from the slope of the plot. The activation energy
16 decreases with the increasing content of triptycene moiety showing that hydroxide ion migration
17 is facilitated by this addition. E_a for TRP-100 and TRP-0 were 16.4 and 18.4 kJ/mol, respectively.
18 This improved performance suggests that adding polymer additives with high free volume is a
19 promising method to achieve higher conductivity for anion exchange membranes.
20
21
22
23
24
25
26
27
28
29
30
31
32
33
34
35
36
37
38
39
40
41
42

43 The difference on conductivity and E_a, of the five samples, prompted small-angle X-ray
44 scattering (SAXS) measurements to quantitatively understand internal domain morphologies.
45 SAXS profiles of the samples with higher triptycene contents (TRP-50, TRP-80 and TRP-100)
46 showed a notable peak in the q range of 0.15 – 0.08 Å⁻¹. Those q ranges are for ionomer peaks,
47 arising from the mean correlation spacing between the hydrophilic water-domains and indicate
48 the size of the ionic clusters within the samples.²² The SAXS data revealed that TRP-100 had
49
50
51
52
53
54
55
56
57
58
59
60

1
2
3 the largest d-spacing, with an internal domain size of 7.44 nm, followed by TRP-80 and TRP-50
4 at 6.28 and 5.08 nm, respectively (Figure 1b). TRP-20 and TRP-0 had relatively featureless
5 scattering profiles from which we cannot extract a d-spacing data. The differently sized internal
6 scattering profiles from which we cannot extract a d-spacing data. The differently sized internal
7 domain morphologies seen from SAXS can be directly observed in Transmission Electron
8 Microscopic (TEM) images. The dark and bright parts of the images respectively correspond to
9 stained hydrophilic methylimidazole functionalized domains and hydrophobic domains that
10 include the additives (Figure 2). Addition of hydrophobic additives induced nano-sized
11 hydrophilic/hydrophobic phase separation with TRP-50, TRP-80 and TRP-100 all clearly
12 showing phase separated morphologies. TRP-100 exhibited a much clearer and larger phase
13 separation than TRP-50, and consistent with the SAXS results TRP-0 and TRP-20 did not
14 display morphological patterns. Thus, higher content of unfunctionalized triptycene in the
15 membrane resulted in the development of phase separation with larger hydrophilic internal
16 domain sizes.



47 **Figure 2.** a-c. TEM images of TRP-50, TRP-80, TRP-100, respectively. Scale for images a-c
48 is given in c.
49

50
51
52 To further understand the membrane structure and characteristics, water uptake and
53 swelling ratios of the membranes were measured. TRP-0 undergoes a 67% water uptake at 20 °C,
54 whereas TRP-100 takes up 1.6-times more water (Figure 3a). Furthermore, although TRP-0's
55
56
57
58
59
60

water uptake increases 87% with a temperature increase from 20 °C to 80 °C, TRP-100 only undergoes a 37% increase of the full range. We attribute this behavior to increased and stable free volume TRP-100, which allows for domain structures that entrap water in the membrane.

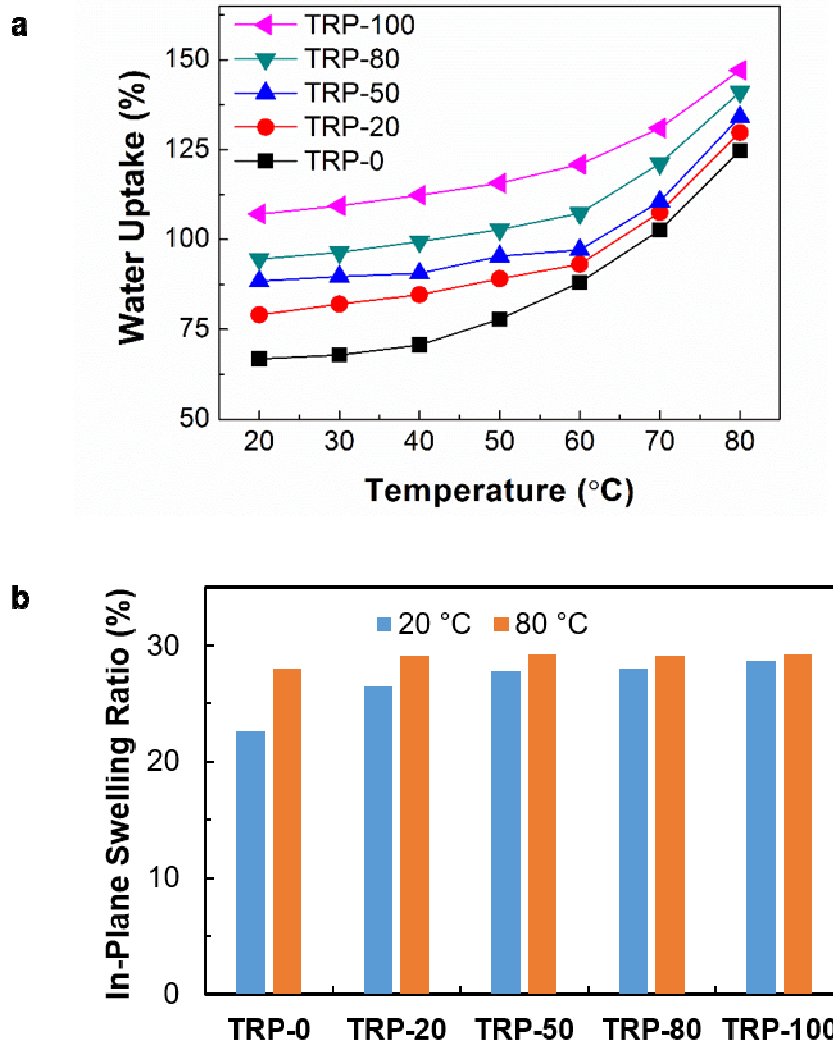


Figure 3. Water uptake (a) and in-plane swelling ratio (b) of samples in the temperature ranges of 20 °C and 80 °C.

The triptycene additives improve the dimensional stability of the samples. By comparing swelling ratios from a dry reference state relative to the membranes in water at 20 °C and 80 °C, dimensional changes of the membranes at various temperatures were observed. Dimensional

1
2
3 stability is necessary to preserve the integrity of the fuel cell under the changing operating
4
5 conditions. Corresponding to the water uptake results, TRP-100 had a small change of swelling
6
7 ratio from 28.7% to 29.2 % for the temperature change from 20 °C to 80 °C (Figure 3b).
8
9 However, TRP-0 had relatively larger change of 22.6% to 28.0% for the same temperature
10
11 change. Improved dimensional stability of TRP-100 over TRP-0 is corroborated from
12
13 mechanical tensile tests wherein TRP-100 has improved tensile strength and a higher Young's
14
15 modulus relative to TRP-0 (Figure S4 and Table S3). Additionally, the thermal stability of the
16
17 membranes as determined by thermal gravimetric analysis were not adversely affected by the
18
19 addition of triptycene additives (Figure S5).
20
21
22
23
24
25
26
27
28
29
30
31
32
33
34
35
36
37
38
39
40
41
42
43
44
45
46
47
48
49
50
51
52
53
54
55
56
57
58
59
60

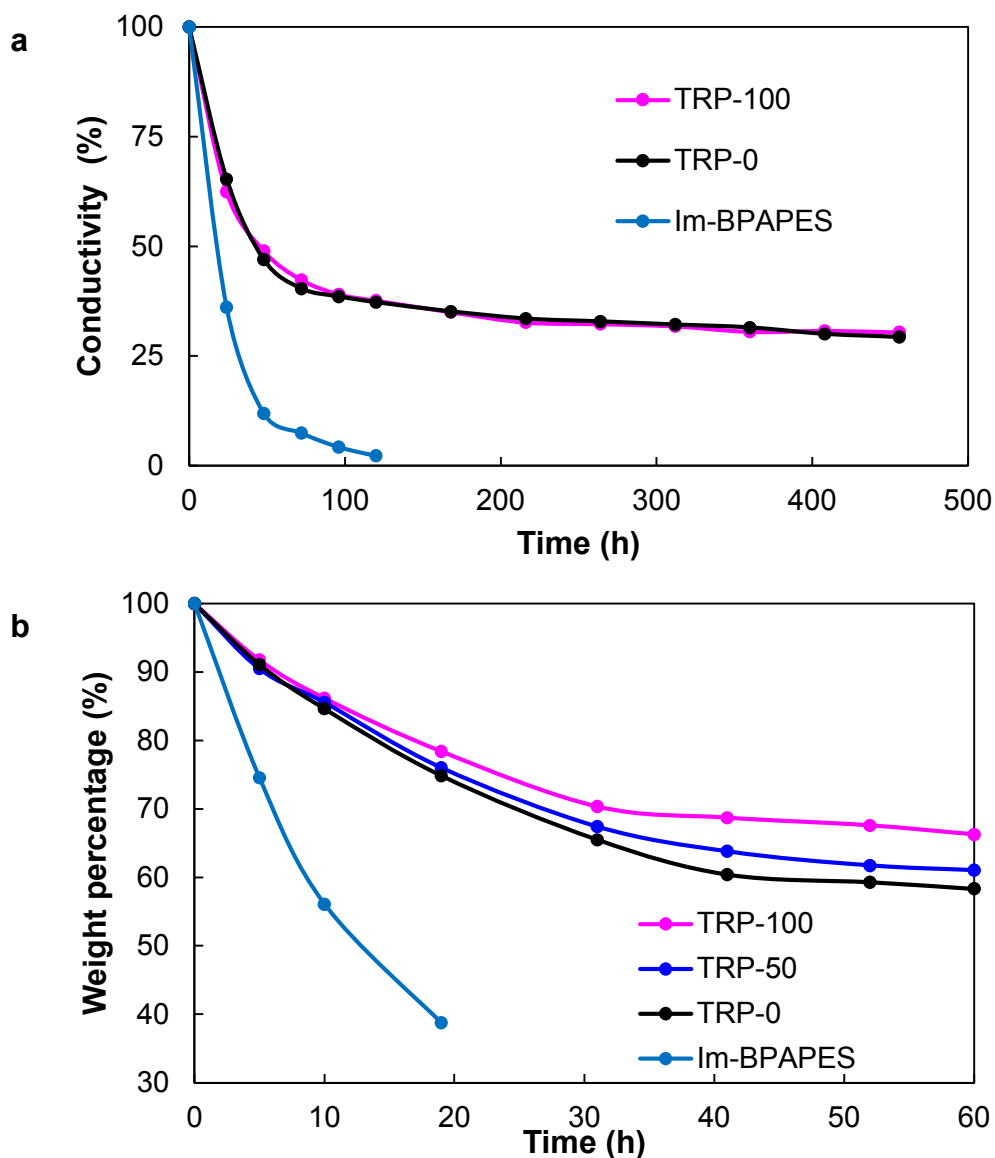


Figure 4. Time dependent hydroxide ion conductivity of the samples. Samples were soaked in 1 M NaOH at 80 °C. Initial IEC for TRP-0 and TRP-100 were 2.40 mmol/g, and Im-BPAPES was 1.83 mmol/g. b, Time dependent oxidative stability of the samples. Samples were soaked in 3% H₂O₂/4 ppm Fe²⁺ solution at 80 °C.

The membranes were soaked in a 1 M NaOH solution at 60 °C to evaluate their alkaline stability. After treating the membranes for the required amount of time, the membranes were washed and soaked in degassed deionized water and the time dependence of the ionic conductivity was determined (Figure 4a). Conductivity of highly functionalized additive-free Im-

1
2
3 BPAPES (IEC = 2.40 mmol/g) decreases rapidly. In addition, these membranes disintegrated as a
4 result of excessive swelling after 120 h, making further measurements unreliable. With additives,
5 an initial sharp decrease in conductivity within the first 72 h was observed as well. However, the
6 conductivity stabilized to a constant value to retain ca. 30% of the original values: 0.0054 S/cm
7 and 0.009 S/cm for TRP-0 and TRP-100, respectively. With more stable cationic groups such as
8 substituted imidazoliums, we are hopeful that the improvements in stability resulting from the
9 additives can be further enhanced and sustained.³¹

10
11
12
13
14
15
16
17
18
19
20 Oxidative stability of the membranes is crucial as long living superoxide anion radicals
21 ($O_2^{\cdot-}$) are often generated under the harsh operating conditions of alkaline fuel cells. $O_2^{\cdot-}$
22 generated could attack the ether linkages and eventually lead to disintegration of the
23 backbones.^{32,33} Thus, membrane stability in strong oxidative condition was simulated by soaking
24 the membrane in Fenton's reagent at an elevated temperature of 80 °C (Figure 4b). Similar to the
25 trend of hydroxide ion conductivity in NaOH solution, weight of Im-BPAPES decreases rapidly
26 within the first 20 hours to the point that the membrane was no longer measureable. On the other
27 hand, masses of membranes with additives decreases gradually and stabilized after 40 h retaining
28 ca. 60 %, 64 % and 69 % of the initial weight of TRP-0, TRP-50 and TRP-100, respectively.
29 Hydroxide conductivity of TRP-100 at 30 °C after the oxidative stability test for 60 h decreased
30 from 0.031 S/cm to 0.012 S/cm, suggesting a loss of functional groups within the membrane.
31 However, the membrane retained fairly high amount of its conductivity, suggesting that the
32 membrane was stable after the initial mass loss.

33
34
35
36
37
38
39
40
41
42
43
44
45
46
47
48
49
50
51
52
53 Addition of free volume promoting triptycene polymers into the anion exchange
54 membranes enhances a number of performance metrics, including higher ionic conductivity,
55
56
57
58
59
60

1
2
3 improved mechanical and chemical stability. The higher ionic conductivity was attributed to
4 additive promoted nanoscale hydrophobic/hydrophilic phase separation. Enhanced mechanical
5 properties are consistent with the triptycene molecules that promote interlocking rigidifying
6 interactions between polymer chains. Further studies using other free-volume promoting
7 molecular building blocks combined with effective strategies for nanoscale phase separation are
8 in order. Our expectation is that these and related strategies will contribute to the development
9 of new generations of high performance anion exchange membranes for electrochemical
10 conversion and storage devices, such as redox-flow batteries, electrodialysis, and high power
11 output fuel cells.
12
13
14
15
16
17
18
19
20
21
22
23
24
25
26
27
28

29 AUTHOR INFORMATION

30 31 32 **Corresponding Author**

33
34
35 *To whom correspondence should be addressed. E-mail: tswager@mit.edu
36
37

38 **Author Contributions**

39
40 The manuscript was written through contributions of all authors. All authors have given approval
41 to the final version of the manuscript. ‡These authors contributed equally.
42
43
44
45

46 **Notes**

47
48
49 There are no conflicts to declare.
50
51

52 **Supporting Information**

53
54
55 Details about materials, synthetic protocols and characterization methods supplied as Supporting
56 Information.
57
58
59
60

ACKNOWLEDGMENT

This work was supported by the Institute for Soldier Nanotechnologies, Abdul Latif Jameel World Water and Food Security Lab (J-WAFS) and a graduate fellowship from Agency of Science Technology and Research, Singapore.

REFERENCES

- (1) Varcoe, J. R.; Slade, R. C. T. Prospects for Alkaline Anion-Exchange Membranes in Low Temperature Fuel Cells. *Fuel Cells* **2005**, *5*, 187–200.
- (2) Merle, G.; Wessling, M.; Nijmeijer, K. Anion Exchange Membranes for Alkaline Fuel Cells: A Review. *J. Memb. Sci.* **2011**, *377*, 1–35.
- (3) Ran, J.; Wu, L.; He, Y.; Yang, Z.; Wang, Y.; Jiang, C.; Ge, L.; Bakangura, E.; Xu, T. Ion Exchange Membranes: New Developments and Applications. *J. Memb. Sci.* **2017**, *522*, 267–291.
- (4) Varcoe, J. R.; Atanassov, P.; Dekel, D. R.; Herring, A. M.; Hickner, M. A.; Kohl, P. A.; Kucernak, A. R.; Mustain, W. E.; Nijmeijer, K.; Scott, K.; Xu, T.; Zhuang, L. Anion-Exchange Membranes in Electrochemical Energy Systems. *Energy Environ. Sci.* **2014**, *7*, 3135–3191.
- (5) Tanaka, M.; Koike, M.; Miyatake, K.; Watanabe, M.; Watanabe, M.; Guay, D.; Hay, A. S.; Wilson, M.; Garzon, F.; Wood, D.; Zelenay, P.; More, K.; Stroh, K.; Zawodzinski, T.; Boncella, J.; McGrath, J. E.; Inaba, M.; Miyatake, K.; Hori, M.; Ota, K.; Ogumi, Z.; Miyata, S.; Nishikata, A.; Siroma, Z.; Uchimoto, Y.; Yasuda, K.; Kimijima, K.; Iwashita, N. Synthesis and

1
2
3 Properties of Anion Conductive Ionomers Containing Fluorenyl Groups for Alkaline Fuel Cell
4 Applications. *Polym. Chem.* **2011**, *2*, 99–106.

5
6
7
8
9 (6) Janarthanan, R.; Horan, J. L.; Caire, B. R.; Ziegler, Z. C.; Yang, Y.; Zuo, X.; Liberatore,
10 M. W.; Hibbs, M. R.; Herring, A. M. Understanding Anion Transport in An Aminated Trimethyl
11 Polyphenylene with High Anionic Conductivity. *J. Polym. Sci. Part B Polym. Phys.* **2013**, *51*,
12 1743–1750.

13
14
15
16
17
18
19 (7) Kim, D. S.; Fujimoto, C. H.; Hibbs, M. R.; Labouriau, A.; Choe, Y.-K.; Kim, Y. S.
20 Resonance Stabilized Perfluorinated Ionomers for Alkaline Membrane Fuel Cells.
21
22
23
24
25
26
27
28
29
30
31
32
33
34
35
36
37
38
39
40
41
42
43
44
45
46
47
48
49
50
51
52
53
54
55
56
57
58
59
60
Macromolecules **2013**, *46*, 7826–7833.

(8) Thomas, O. D.; Soo, K. J. W. Y.; Peckham, T. J.; Kulkarni, M. P.; Holdcroft, S. A Stable
Hydroxide-Conducting Polymer. *J. Am. Chem. Soc.* **2012**, *134*, 10753–10756.

(9) Guo, T. Y.; Zeng, Q. H.; Zhao, C. H.; Liu, Q. L.; Zhu, A. M.; Broadwell, I. Quaternized
Polyepichlorohydrin/PTFE Composite Anion Exchange Membranes for Direct Methanol
Alkaline Fuel Cells. *J. Memb. Sci.* **2011**, *371*, 268–275.

(10) Robertson, N. J.; Kostalik, H. A.; Clark, T. J.; Mutolo, P. F.; Abruña, H. D.; Coates, G.
W. Tunable High Performance Cross-Linked Alkaline Anion Exchange Membranes for Fuel Cell
Applications. *J. Am. Chem. Soc.* **2010**, *132*, 3400–3404.

(11) Cotter, R. J. *Engineering Plastics: A Handbook of Polyarylethers*; Gordon and Breach,
London, 1995.

1
2
3 (12) Arges, C. G.; Ramani, V. Two-Dimensional NMR Spectroscopy Reveals Cation-
4 Triggered Backbone Degradation in Polysulfone-Based Anion Exchange Membranes *Proc. Natl.*
5
6 *Acad. Sci. U. S. A.* **2013**, *110*, 2490-2495.
7
8

9
10
11 (13) Wang, J.; He, G.; Wu, X.; Yan, X.; Zhang, Y.; Wang, Y.; Du, L. Crosslinked Poly (ether
12 ether ketone) Hydroxide Exchange Membranes with Improved Conductivity. *J. Memb. Sci.* **2014**,
13
14 *459*, 86–95.
15
16

17
18
19 (14) Lai, A. N.; Wang, L. S.; Lin, C. X.; Zhuo, Y. Z.; Zhang, Q. G.; Zhu, A. M.; Liu, Q. L.
20 Benzylmethyl-Containing Poly(arylene ether nitrile) As Anion Exchange Membranes for
21 Alkaline Fuel Cells. *J. Memb. Sci.* **2015**, *481*, 9–18.
22
23
24

25
26
27 (15) Ye, Y.; Elabd, Y. A. Relative Chemical Stability of Imidazolium-Based Alkaline Anion
28 Exchange Polymerized Ionic Liquids. *Macromolecules*, **2011**, *44*, 8494–8503.
29
30

31
32
33 (16) Zhang, F.; Zhang, H.; Qu, C. Imidazolium Functionalized Polysulfone Anion Exchange
34 Membrane for Fuel Cell Application. *J. Mater. Chem.* **2011**, *21*, 12744–12752.
35
36

37
38
39 (17) Li, N.; Leng, Y.; Hickner, M. A.; Wang, C.-Y. Highly Stable, Anion Conductive, Comb-
40 Shaped Copolymers for Alkaline Fuel Cells. *J. Am. Chem. Soc.* **2013**, *135*, 10124–10133.
41
42

43
44 (18) Tanaka, M.; Fukasawa, K.; Nishino, E.; Yamaguchi, S.; Yamada, K.; Tanaka, H.; Bae,
45 B.; Miyatake, K.; Watanabe, M. Anion Conductive Block Poly(arylene ether)s: Synthesis,
46 Properties, and Application in Alkaline Fuel Cells. *J. Am. Chem. Soc.* **2011**, *133*, 10646–10654.
47
48
49

50
51
52 (19) Xu, P. Y.; Zhou, K.; Lu, G.; Qiu, H.; Zhang, G.; Zhu, A. M.; Liu, Q. L. Effect of
53 Fluorene Groups on the Properties of Multiblock Poly(arylene ether sulfone)s-Based Anion-
54 Exchange Membranes. *ACS Appl. Mater. Interfaces*, **2014**, *6*, 6776–6785.
55
56
57
58
59
60

1
2
3 (20) Lee, K. H.; Cho, D. H.; Kim, Y. M.; Moon, S. J.; Seong, J. G.; Shin, D. W.; Sohn, J.-Y.;
4 Kim, J. F.; Lee, Y. M.; Guiver, M. D.; Lim, T.-H.; Zhuang, L.; Hill, A. J.; Guiver, M. D.; Lee, Y.
5 M. Highly Conductive and Durable Poly(arylene ether sulfone) Anion Exchange Membrane with
6 End-Group Cross-Linking. *Energy Environ. Sci.* **2017**, *10*, 275–285.
7
8

9
10
11
12
13 (21) Long, L.; Wang, S.; Xiao, M.; Meng, Y. Polymer Electrolytes for Lithium Polymer
14 Batteries. *J. Mater. Chem. A*, **2016**, *4*, 10038-10069.
15
16

17
18
19 (22) Shin, D. W.; Guiver, M. D.; Lee, Y. M. Hydrocarbon-Based Polymer Electrolyte
20 Membranes: Importance of Morphology on Ion Transport and Membrane Stability. *Chem. Rev.*
21 **2017**, *117*, 4759–4805.
22
23

24
25 (23) Swager, T. M. Iptycenes in the Design of High Performance Polymers. *Acc. Chem. Res.*
26 **2008**, *41*, 1181–1189.
27
28

29
30 (24) Yang, J.-S.; Swager, T. M. Fluorescent Porous Polymer Films as TNT Chemosensors:
31 Electronic and Structural Effects. *J. Am. Chem. Soc.* **1998**, *120*, 11864–11873.
32
33

34
35 (25) Long, T. M.; Swager, T. M. Molecular Design of Free Volume as a Route to Low- κ
36 Dielectric Materials. *J. Am. Chem. Soc.* **2003**, *125*, 14113–14119.
37
38

39
40 (26) Tsui, N. T.; Torun, L.; Pate, B. D.; Paraskos, A. J.; Swager, T. M.; Thomas, E. L.
41 Molecular Barbed Wire: Threading and Interlocking for the Mechanical Reinforcement of
42 Polymers. *Adv. Funct. Mater.* **2007**, *17*, 1595–1602.
43
44

45
46 (27) Zhao, Z.; Gong, F.; Zhang, S.; Li, S. Poly(arylene ether sulfone)s Ionomers Containing
47 Quaternized Triptycene Groups for Alkaline Fuel Cell. *J. Power Sources* **2012**, *218*, 368–374.
48
49
50
51

1
2
3 (28) Xu, H.; Fang, J.; Guo, M.; Lu, X.; Wei, X.; Tu, S. Novel Anion Exchange Membrane
4 Based on Copolymer of Methyl Methacrylate, Vinylbenzyl Chloride and Ethyl Acrylate for
5 Alkaline Fuel Cells. *J. Memb. Sci.* **2010**, *354*, 206–211.
6
7

8
9
10
11 (29) Lin, B.; Dong, H.; Li, Y.; Si, Z.; Gu, F.; Yan, F. Alkaline Stable C2-Substituted
12 Imidazolium-Based Anion-Exchange Membranes. *Chem. Mater.* **2013**, *25*, 1858–1867.
13
14

15
16
17 (30) Weiber, E. A.; Jannasch, P. Polysulfones with Highly Localized Imidazolium Groups for
18 Anion Exchange Membranes. *J. Memb. Sci.* **2015**, *481*, 164–171.
19
20

21
22 (31) Hugar, K. M.; Kostalik, H. A.; Coates, G. W. Imidazolium Cations with Exceptional
23 Alkaline Stability: A Systematic Study of Structure–Stability Relationships *J. Am. Chem. Soc.*
24 **2015**, *137*, 8730-8737.
25
26
27

28
29
30 (32) Zhang, Y.; Parrondo, J.; Sankarasubramanian, S.; Ramani, V. Detection of Reactive
31 Oxygen Species in Anion Exchange Membrane Fuel Cells using In Situ Fluorescence
32 Spectroscopy. *ChemSusChem* **2017**, *10*, 3056-3062.
33
34
35
36

37
38 (33) Kitajima, N.; Fukuzumi, S.; Ono, Y. Formation of Superoxide Ion During the
39 Decomposition of Hydrogen Peroxide on Supported Metal Oxides *J. Phys. Chem.* **1978**, *82*,
40 1505-1509.
41
42
43
44
45
46
47
48
49
50
51
52
53
54
55
56
57
58
59
60

Graphic for manuscript

